Magn Reson Med Sci 2021; 20; 91–98
doi:10.2463/mrms.mp.2020-0030
Published Online: April 15, 2020

MAJOR PAPER

Intracranial Distribution of Intravenously Administered Gadolinium-based Contrast Agent over a Period of 24 Hours: Evaluation with 3D-real IR Imaging and MR Fingerprinting

Shinji Naganawa[1*], Rintaro Ito[1], Yutaka Kato[1], Hisashi Kawai[1], Toshiaki Taoka[1], Tadao Yoshida[2], Katsuya Maruyama[3], Katsutoshi Murata[3], Gregor Körzdörfer[4], Josef Pfeuffer[4], Mathias Nittka[4], and Michihiko Sone[2]

Purpose: To evaluate the feasibility for the detection of slight contrast effects after intravenous administration of single dose gadolinium-based contrast agent (IV-SD-GBCA), the time course of the GBCA distribution up to 24 h was examined in various fluid spaces and brain parenchyma using 3D-real IR imaging and MR fingerprinting (MRF).

Methods: Twenty-four patients with a suspicion of endolymphatic hydrops were scanned at pre-administration and at 10 min, 4 and 24 h post-IV-SD-GBCA. 3D-real IR images and MRF at the level of the internal auditory canal were obtained. The signal intensity on the 3D-real IR image of the cerebrospinal fluid (CSF) in the cerebellopontine angle cistern (CPA), Sylvian fissure (Syl), lateral ventricle (LV), and cochlear perilymph (CPL) was measured. The T_1 and T_2 values of cerebellar gray (GM) and white matter (WM) were measured using MRF. Each averaged value at the various time points was compared using an analysis of variance.

Results: The signal intensity on the 3D-real IR image in each CSF region peaked at 4 h, and was decreased significantly by 24 h ($P < 0.05$). All patients had a maximum signal intensity at 4 h in the CPA, and Syl. The mean CPL signal intensity peaked at 4 h and decreased significantly by 24 h ($P < 0.05$). All patients but two had a maximum signal intensity at 4 h. Regarding the T_1 value in the cerebellar WM and GM, the T_1 value at 10 min post-IV-GBCA was significantly decreased compared to the pre-contrast scan, but no significant difference was observed at the other time points. There was no significant change in T_2 in the gray or white matter at any of the time points.

Conclusion: Time course of GBCA after IV-SD-GBCA could be evaluated by 3D-real IR imaging in CSF spaces and in the brain by MRF.

Keywords: *magnetic resonance imaging, magnetic resonance fingerprinting, gadolinium, glymphatic system*

Introduction

Several studies using heavily T_2-weighted 3D-FLAIR imaging have reported changes in the distribution of intravenously administered gadolinium-based contrast agents (GBCAs) in various liquid cavities over time.[1–5] One study examined up to 6 h post-administration[4] and another one investigated changes up to 24 h post-administration using heavily T_2-weighted 3D-FLAIR imaging.[1]

Heavily T_2-weighted 3D-FLAIR imaging is quite sensitive for the detection of low concentrations of GBCA in fluid.[6,7] However, with heavily T_2-weighted 3D-FLAIR imaging, a paradoxical signal drop due to the GBCA distribution can occur during the longitudinal recovery period after the application of the inversion pulse, and prior to passing the null point.[3,8] In addition, not only heavily T_2-weighted 3D-FLAIR imaging, but also all inversion recovery methods in general, might not apply a completely uniform inversion pulse within the slab volume. Thus, there may be areas where the complete spin inversion does not

[1]Department of Radiology, Nagoya University Graduate School of Medicine, Aichi, Japan
[2]Department of Otorhinolaryngology, Nagoya University Graduate School of Medicine, Aichi, Japan
[3]Siemens Healthcare KK, Tokyo, Japan
[4]Siemens Healthcare GmbH, Erlangen, Germany
[*]Corresponding author: Department of Radiology, Nagoya University Graduate School of Medicine, 65 Tsurumai-cho, Shouwa-ku, Nagoya, Aichi 466-8550, Japan. Phone: +81-52-744-2327, Fax: +81-52-744-2335, E-mail: naganawa@med.nagoya-u.ac.jp

Received: February 14, 2020 | Accepted: March 20, 2020

occur. For example, if the inversion time is set to null for the cerebrospinal fluid (CSF) in the lateral ventricles, the CSF in other regions might not be sufficiently nulled. Thus, there may be some fluid-containing voxels before passing the null point in FLAIR images that were adjusted to a null point of a different CSF region. At such sites, the paradoxical signal drops due to the GBCA distribution described above can occur with magnitude reconstruction. In order to overcome this problem, the use of 3D inversion recovery with real reconstruction (3D-real IR) imaging is preferable for the determination of subtle contrast effects in fluid.[3,8]

Currently, 3D-real IR imaging with heavily T_2 weighting is used for the detection of small amounts of GBCA in CSF spaces and the labyrinthine perilymph.[3,8] In this method, since the degree of T_2 weighting is strong, almost no brain parenchymal signal is obtained. Therefore, the contrast effect in the brain parenchyma cannot be evaluated.

Alternatively, one study indicated that MR fingerprinting (MRF) of 3D-real IR imaging can detect T_1 and T_2 shortening in CSF spaces with distinct contrast enhancement after intravenous injection of GBCA.[9] MRF can also be used to evaluate the changes of T_1 and T_2 in brain parenchyma.[10–13] There is an advantage in that the dynamic range is larger using MRF than for 3D-real IR imaging alone.

Various studies have shown that GBCAs distribute in various fluid spaces such as the CSF, the perilymph of the inner ear, the perivascular spaces of the basal ganglia, the meningeal lymphatics and the brain parenchyma after IV administration.[1–5,9,14–20]

The pattern for the intracranial distribution of intravenously administered GBCA might be associated with aging, blood–brain barrier (BBB) integrity, function of glymphatic system, and renal function.[2,3,21,22] The glymphatic system is the waste clearance system of the brain and has attracted much attention from a wide range of investigators.[23–25] Establishment of a method for the evaluation of the glymphatic system is a hot research topic in the neuroscience field.[26] Currently, the distribution patterns of intravenously administered GBCA in various fluid spaces of humans are under intense investigation as the first step of the glymphatic system and as a measure of BBB integrity.[1,25,27] For the evaluation of the glymphatic system in brain parenchyma, an intrathecal administration of a small dose of GBCA (IT-GBCA) is used by some investigators.[23,28] However, intrathecal administration of GBCA is usually contraindicated in a clinical setting.[29] If we could detect the presence of intravenously administered GBCA in brain parenchyma, the evaluation of glymphatic system in clinical setting might be feasible.

The purpose of this study was to evaluate the feasibility of detecting slight contrast effects in CSF and brain parenchyma after intravenous administration of single dose GBCA (IV-SD-GBCA). For this purpose, we used both 3D-real IR imaging[3,8,9,14] and MRF[9,10,30] pre- and post-intravenous injection of GBCA through 24 h to evaluate the contrast in the CSF, cochlear perilymphatic space, and in the cerebellar white and gray matter. This study represents a next step for research of the glymphatic system in a clinical setting.

Materials and Methods

Patients

The subjects were 24 patients suspected of endolymphatic hydrops (nine women and 15 men, age: 23–80, median age: 55). In all cases, the estimated glomerular filtration rate was 50 mL/min/1.73 m^2 or greater. There were no cases with brain tumors or large cerebral infarctions. The ethical committee of our institution approved this study. Written informed consent was obtained from all patients.

MR imaging

The images were obtained pre-administration, and at 10 min, 4 and 24 h post-intravenous administration of a single dose (0.1 mmol/kg) of macrocyclic GBCA (gadobutrol, Bayerpharm, Osaka, Japan). A 3T MR scanner (MAGNETOM Skyra, Siemens Healthcare, Erlangen, Germany) with a 32-channel head coil was used. The detailed parameters for the 3D-real IR imaging and 2D-MRF were similar to a previous study, but the measurement time for the 2D-MRF was reduced from 41 to 21 s per slice by reducing the number of echoes from 3000 to 1500.[9] Briefly, for 3D-real IR imaging we obtained 256 axial slices with 1 mm thickness covering the entire brain, as well as axial 2D-MRF (5 mm slice thickness) at the level of the inner ear canal.

The prototype 2D-MRF sequence was based on an FISP acquisition scheme, that uses a spiral readout trajectory, inversion recovery pulse, variable TR, and variable flip angles. The slice thickness for this acquisition was 5 mm and had a square field of view of 300 mm. The matrix size was 256 × 256. The scan parameters included an echo time of 2.0 ms and an inversion time of 20.6 ms. The repetition time ranged from 12.1 to 15.0 ms, and the flip angle ranged from 0° to 74°. Each echo encoded an image by a single spiral readout with a variable-density *k*-space trajectory (24- to 48-fold under-sampling),[31] and the spiral trajectory was rotated by 82.5° for each repetition time to improve the temporal incoherence of the under-sampling artifacts.[32] To compensate for the inhomogeneity of the RF-field (B_1^+), an automated field correction was applied. Before the actual MRF scan was started, an RF-field-mapping sequence was triggered.[33] After acquisition of the MRF data, the scanner automatically performed pattern recognition between the calculated dictionary and the measured time course. One slice of MRF at the level of internal auditory canal was obtained and analyzed.

The scan time for the 3D-real IR imaging was 10 min per volume and the MRF was 21 s per slice. Detailed parameters of 3D-real IR imaging are shown in Table 1. Slice position for 3D-real IR imaging and MRF was co-registered between time points using a scanner-equipped automatic alignment function.[34]

Table 1 Pulse sequence parameters

Sequence name	Type	Repetition time (ms)	Echo time (ms)	Inversion time (ms)	Flip angle (°)	Section thickness/ gap (mm)	Pixel size (mm)	Number of slices	Echo train length	Field of view (mm)	Matrix size	Number of excitations	Scan time (min)
3D-real IR	SPACE with inversion pulse	15130	549	2700	90/ constant145	1/0	0.5 × 0.5	256	256	165 × 196	324 × 384	1	10

GRAPPA, (GeneRalized Autocalibrating Partial Parallel Acquisition) × 3 for real IR; SPACE, sampling perfection with application-optimized contrasts using different flip angle evolutions; 3D-real IR, 3D inversion recovery with phase sensitive reconstruction (real reconstruction).

This sequence utilizes a frequency selective fat suppression pre-pulse, non-slab selective excitation pulse, and non-slab selective inversion pulse.

3D slab is set in an axial orientation.

Image analysis

On the 3D-real IR images, 3 mm diameter circular regions of interest (ROIs) were placed in the bilateral cerebellopontine angle cistern, the bilateral trigone of the lateral ventricle, and the bilateral Sylvian fissure, while avoiding brain tissue, cranial nerves, choroid plexus and blood vessels, and the CSF signal intensity was measured. The signal intensity of the perilymph in the left and right cochlear basal turn was also measured. The perilymph signal intensity was measured by manually surrounding the scala tympani in the basal turn of cochlea. Examples of the ROI placement are shown in Fig. 1.

For MRF, T_1 and T_2 were measured by placing a 10-mm circular ROI in the gray (i.e. cerebellar hemispheres) and white (i.e. middle cerebellar peduncles) matter of the left and right cerebellum, while avoiding the CSF and blood vessels. Examples of the ROI placement are shown in Fig. 2.

For each CSF and perilymph signal intensity measurement on the 3D-real IR images as well as the T_1 and T_2 values from the cerebellar white and gray matter on MRF, the values of the left and the right were averaged. Averaged values at all time points were compared using an analysis of variance. A Bonferroni correction was performed for multiple comparisons. The T_1 ratio (T_1 value at 10 min divided by that at pre-contrast) was calculated and compared between gray and white matter using a Student's *t*-test. We used 5% as a threshold to determine statistical significance. The software R (version 3.3.2, R Foundation for Statistical Computing, Vienna, Austria, https://www.R-project.org/) was used for the statistical analyses.

Results

The mean cochlear perilymph signal intensity peaked at 4 h and decreased significantly by 24 h ($P < 0.05$). All patients but two had a maximum signal intensity at 4 h.

There was no significant difference in signal intensity at pre-administration and 10 min post-contrast, and all other time points were significantly different from pre-contrast (Figs. 3 and 4).

The mean signal intensity of 3D-real IR from each CSF compartment peaked at 4 h, and it decreased significantly by 24 h ($P < 0.05$). All patients had a peak signal intensity at 4 h in the cerebellopontine angle cistern, and the Sylvian fissure. All patients but six had a peak signal intensity at 4 hours in the lateral ventricle (Figs. 3 and 4). The mean signal intensity at 24 h remained significantly higher than pre-contrast images in the cerebellopontine angle cistern and the Sylvian fissure.

In the cerebellar gray and white matter, a significant shortening of the mean T_1 at 10 min post-GBCA

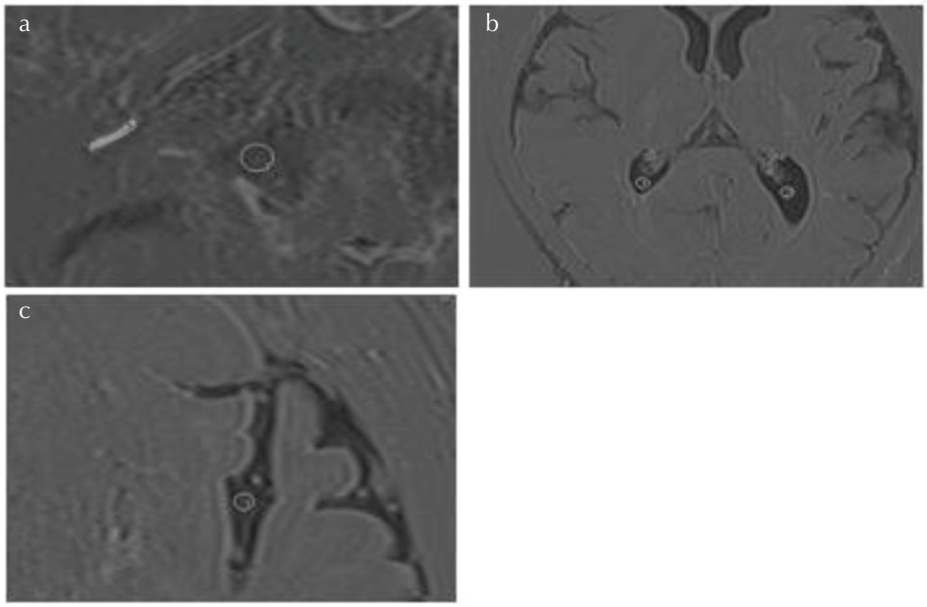

Fig. 1 An example of the region of interest (ROI) placement for signal intensity measurements on 3D-real IR images. Values from the right and left sides were averaged. (**a**) For the cerebrospinal fluid (CSF) in the cerebellopontine angle cistern, a circular ROI was drawn (ROI#1). For the cochlear perilymph, the scala tympani in the basal turn of the cochlea was manually contoured (ROI#2). (**b**) For the CSF in the lateral ventricle, a circular ROI was drawn posterior to the choroid plexus bilaterally (ROI#1 and #2). (**c**) For the CSF in the Sylvian fissure, a circular ROI was drawn in the fissure avoiding blood vessels (ROI#1 for the left Sylvian fissure).

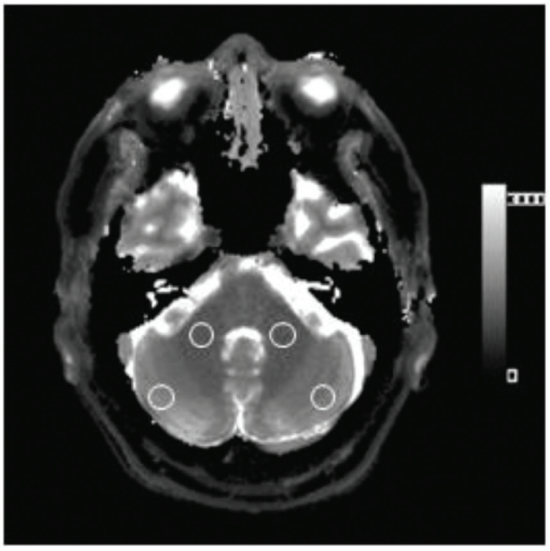

Fig. 2 An example of the region of interest (ROI) placement on the T_1 map by MR fingerprinting. Circular ROIs were manually placed in both the cerebellar gray matter (cerebellar hemisphere) and the white matter (i.e. middle cerebellar peduncle). The ROIs were placed to avoid the CSF. The T_1 values from both sides were averaged. These ROIs were copied and pasted onto the T_2-map.

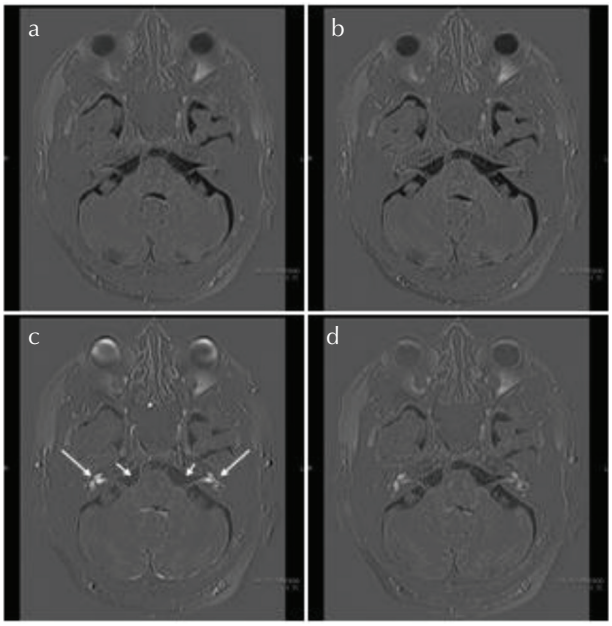

Fig. 3 An example of 3D-real IR images at pre-administration (**a**), 10 min (**b**), 4 (**c**) and 24 h (**d**) post-intravenous administration of the gadolinium-based contrast agent. The perilymph in both sides of the cochlea was most strongly enhanced at 4 h (arrows). The signal intensity of the cerebrospinal fluid in the cerebellopontine angle cistern was highest at 4 h (short arrows).

administration was observed as compared to the pre-contrast scan, but no significant differences were found for other time point comparisons (Fig. 5a and 5b). In all patients, T_1 was decreased at 10 min in both gray and white matter compared to that in the pre-contrast image. The mean T_1 ratio (T_1 value at 10 min divided by the value at pre-contrast) was 0.934 ± 0.02 for gray matter and 0.963 ± 0.01 for white matter. This ratio was significantly less in the gray matter ($P < 0.01$).

There was no significant change in the mean T_2 value over time in either gray or white matter (Fig. 5c and 5d).

Discussion

CSF enhancement

It was reported that the intravenously administered GBCA distributes in CSF. The GBCA leaks from the impaired portion of the BBB, the peripheral part of the cranial nerves, choroid plexus, circumventricular organs, and subarachnoid vessels.[2–5,14,20,25,27] It has been reported that the CSF signal

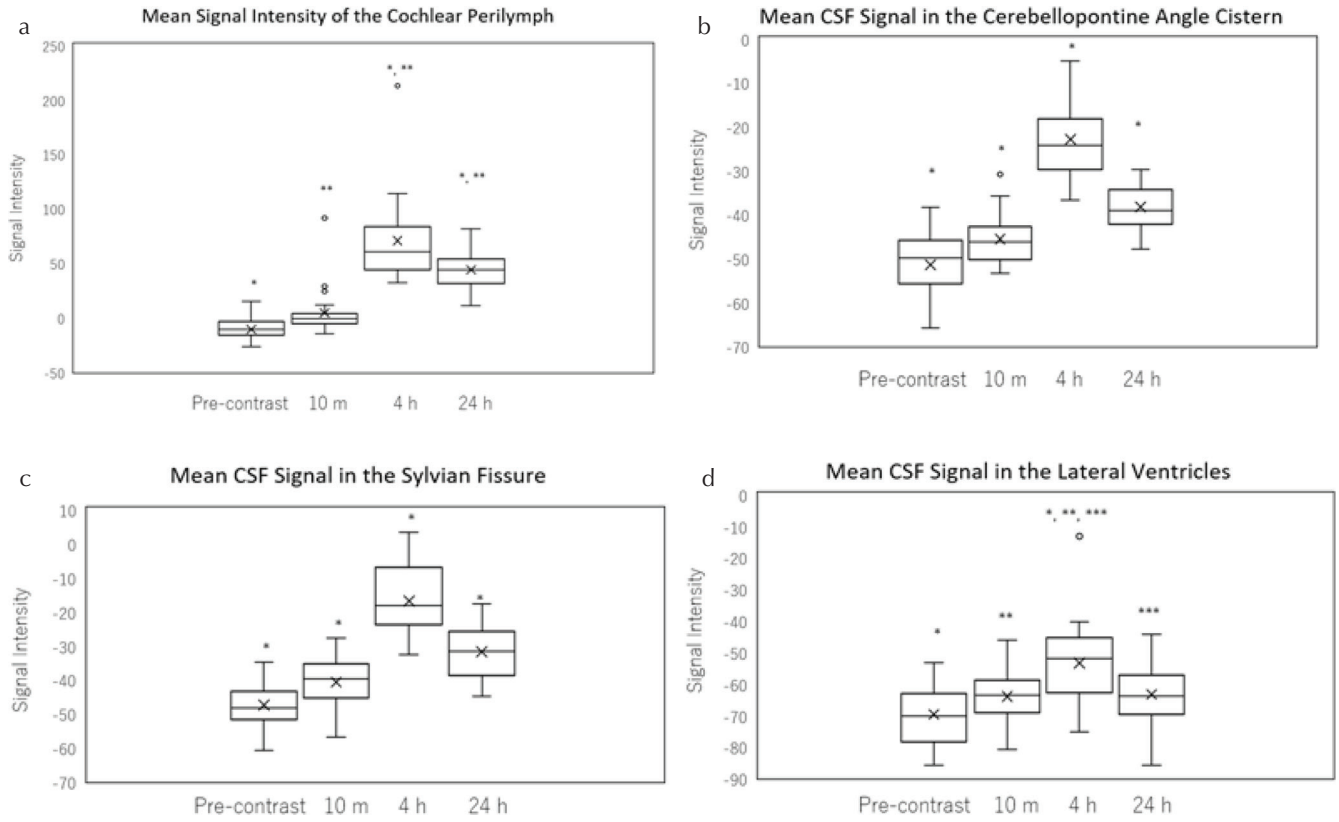

Fig. 4 A box-and-whisker plot of the signal intensity of the cochlear perilymph (**a**), cerebrospinal fluid (CSF) in the cerebellopontine angle cistern (**b**), CSF in the Sylvian fissure (**c**), CSF in the lateral ventricle (**d**) pre-, 10 min, 4 and 24 h post-intravenous administration of gadolinium-based contrast agent on the 3D-real IR images. The lower side of the rectangle is the first quartile (25th percentile value) and the upper side is the 75th percentile value. The horizontal line in the rectangle is the median. The horizontal line under the whisker indicates the 10th percentile value, and the horizontal line above the whisker indicates the 90th percentile value. The cross sign in the rectangle is the mean. (**a**) The mean signal intensity of the cochlear perilymph was highest at 4 h compared to the other time points ($P < 0.01$). The mean signal intensity was significantly higher at 24 h compared to that at pre- and 10 min post-administration ($P < 0.01$). *, **: Significant difference. (**b**) The mean signal intensity of the CSF in the cerebellopontine angle cistern was highest at 4 h compared to all other time points ($P < 0.01$). There was a significant difference between all paired scans. *: Significant difference. (**c**) The mean signal intensity of the CSF in the Sylvian fissure was highest at 4 h compared to all other time points ($P < 0.01$). There was a significant difference between all paired scans. *: Significant difference. (**d**) The mean signal intensity of the CSF in the lateral ventricle was highest at 4 h compared to all other time points ($P < 0.01$). There was no significant difference between the other paired scans. *, **, ***: Significant difference.

intensity in the lateral ventricles and the prepontine cistern was decreased at 24 h compared to 3 h post-administration of GBCA.[1] Decreased enhancement in the CSF at 24 h is consistent with the results of the present study. Leakage of IV-GBCA into the CSF might be affected by various conditions. An effect of age on IV-GBCA leakage into the CSF has been reported.[3] In addition, an association of white matter degeneration and the degree of GBCA distribution in the CSF has also been documented.[1] A correlation of IV-GBCA leakage into the CSF with aging, white matter degeneration, BBB disruption and other pathophysiological conditions would be interesting for future research. The drainage of GBCA from CSF is also important issue in the research of the glymphatic system.[23] The perivascular space, subpial space around cortical vein and meningeal lymphatics might be working as a part of the drainage pathway.[2,3,9,14]

Cochlear perilymph signal intensity

A previous study found that the signal intensity of the cochlear perilymph was decreased at 6 h compared to 4 h post-IV-GBCA in a small number of healthy subjects.[35] In another study, serial scans post-IV-GBCA were carried out in healthy subjects.[4] The cochlear perilymph and the CSF in the internal auditory canal and ambient cistern showed no significant differences between 3 and 4.5 h, and between 4.5 and 6 h post-administration. Further studies are necessary to define the time of peak enhancement in the CSF and perilymph under various conditions.

A recent report indicated that the cochlear perilymph signal intensity was increased at 24 h in healthy subjects compared to 3 h.[1] In the present study, the cochlear perilymph signal intensity was decreased slightly at 24 h compared to 4 h. Also in the previous study, the cochlear perilymph signal intensity tended to be higher in patients with white matter degeneration.[1] In the present study, no evaluation for white

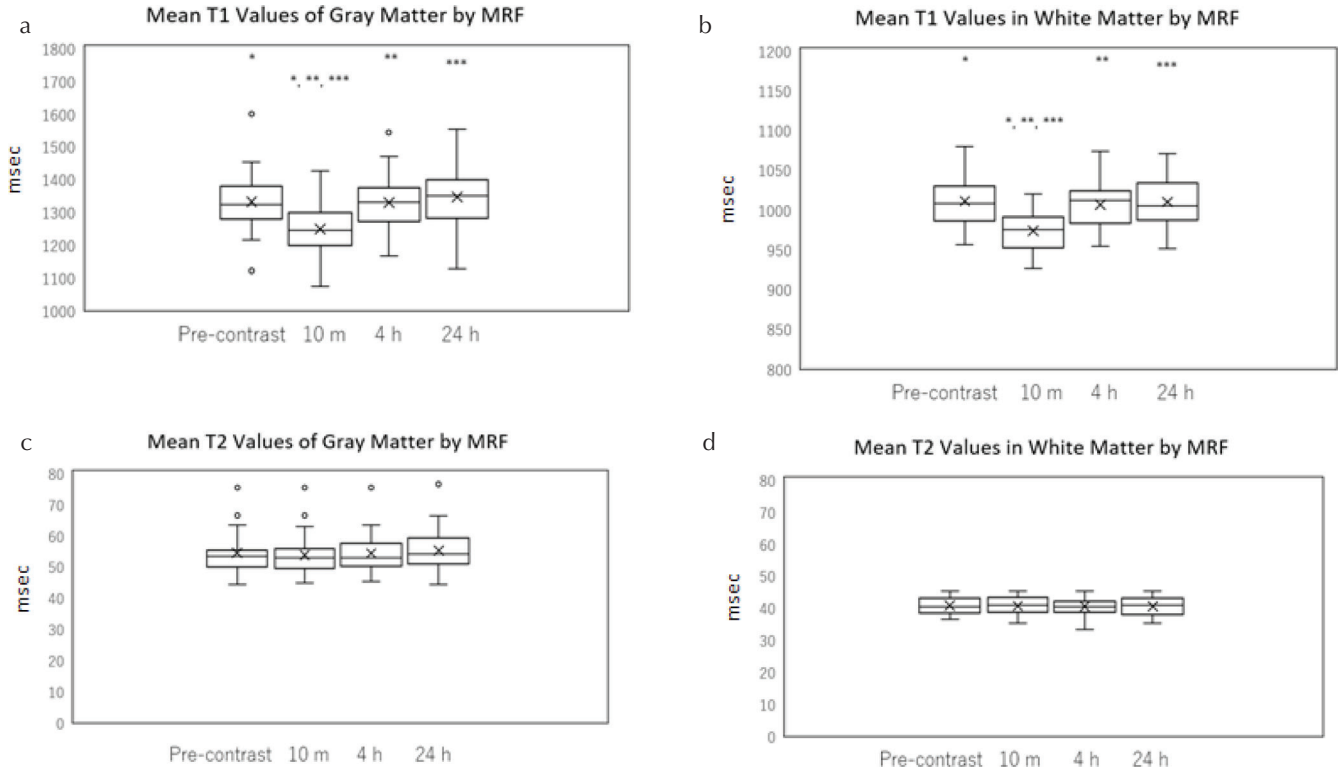

Fig. 5 A box-and-whisker plot of the T_1 and T_2 values in cerebellar gray and white matter for pre-administration, and 10 min, 4 and 24 h post-intravenous administration of gadolinium-based contrast agent as measured by MR fingerprinting (MRF). T_1 of the gray matter (**a**), T_1 of the white matter (**b**), T_2 of the gray matter (**c**), T_2 of the white matter (**d**). The mean T_1-value of gray and white matter at 10 min was significantly smaller than that at all the other time points (**a** and **b**). *, **, ***: Significant difference. There was no significant change in the mean T_2 value over time in either gray or white matter (**c** and **d**). The lower side of the rectangle is the first quartile (25th percentile value) and the upper side is the 75th percentile value. The horizontal line in the rectangle is the median. The horizontal line under the whisker indicates the 10th percentile value, and the horizontal line above the whisker indicates the 90th percentile value. The cross sign in the rectangle is the mean.

matter lesions in the brain was performed, and all patients had a suspicion of endolymphatic hydrops. The reason for the difference in the results between the present study and the previous study[1] is not known, but may be due to differences in the patient groups as well as the scan timing (i.e. 3 vs. 4 h).

Brain parenchyma

For the evaluation of glymphatic function in human subjects, a small dose of IT-GBCA can be administered.[28,36–40] The distribution and clearance of IT-GBCA in brain parenchyma was found to be significantly different between control subjects and idiopathic normal pressure hydrocephalus patients.[40] However, the distribution pattern of IT-GBCA in the brain has a large inter-individual variability, therefore an individual evaluation of glymphatic function by IT-GBCA is difficult.

However, IV-GBCA can also be difficult to interpret, because not only glymphatic function, but also renal function and BBB integrity contribute to the distribution.

It has been demonstrated in animal experiments that the presence of gadolinium contrast in brain parenchyma may be seen with both linear- and macrocyclic-type agents at 24 h after intravenous administration.[20] It has been further clarified that gadolinium contrast agents administered intravenously are distributed in cerebrospinal fluid in healthy subjects.[4,5,41] It has also been shown that gadolinium contrast agents in the cerebrospinal fluid spaces are transferred to brain parenchyma in animals and humans.[20,28,29,37,42]

Thus, if gadolinium contrast is present in cerebrospinal fluid, it will also be present in brain parenchyma. However, in the present study it was found that MRF could not detect the presence of gadolinium contrast that may have transferred from the cerebrospinal fluid spaces into the brain parenchyma after intravenous administration at 4 or 24 h, probably due to the lack of enough sensitivity to trace amounts of GBCA in brain parenchyma. The T_1 shortening in the brain parenchyma at 10 min post-intravenous administration is mainly presumed to be due to the presence of contrast in the blood pool, and not mainly due to GBCA in the interstitial spaces of the brain parenchyma.[22,43,44] To separately evaluate the intravascular versus interstitial components for the presence of GBCA, we might need additional information such as the cerebral blood volume and intravascular concentration of the GBCA. The mean T_1 ratio (i.e. T_1 value at 10 min divided by that at pre-contrast) was larger in white matter than in gray matter. This may reflect the difference of cerebral blood volume between gray and white matter.

We still do not know the precise concentration of GBCA in the cerebellar white and gray matter at 4 and 24 h post-IV-GBCA. Additional scan intervals should be applied in a future study to detect the change in T_1 for the brain parenchyma after IV-GBCA. We might also need to improve the sensitivity of MRF to very low concentration GBCA in brain parenchyma.

We believe that some portion of the GBCA was distributed in the brain parenchyma after intravenous administration even with an intact blood brain barrier. If detected by MRF at some other scan timing, it may be due to a complex mix of BBB leakiness and blood–CSF barrier permeability, as well as clearance or drainage from the brain (i.e. glymphatic function). The results of the present study provide basic data for future research. In the present study, we observed the change over time of the IV-GBCA distribution in the CSF space using 3D-real IR imaging. The CSF signal intensity may be affected not only by glymphatic function, but also by BBB integrity and renal function. Thus, the change in CSF signal intensity over time post-IV-GBCA may be a potential biomarker for glymphatic function.

Limitations of the study

This study has some limitations. We included only a small number of patients with the suspicion of endolymphatic hydrops. Further study including a larger number of patients and healthy volunteers is necessary. Scan timing was limited to only four time points to avoid too much burden on the patients. To obtain more time points, the scan time might need to be much shorter to reduce the time burden on the participants. The number of slices for MRF was limited in this study due to the time constraint. 3D-MRF covering whole brain[45,46] might be beneficial to analyze a larger brain region.

Conclusion

The presence of GBCA in various CSF compartments and in the cochlear perilymph was detected most appreciably by 3D-real IR imaging at 4 h post-IV-SD-GBCA. The presence of GBCA in the brain could be detected at 10 min post-IV-SD-GBCA, but could not be detected at 4 and 24 h post-IV-SD-GBCA by MRF.

Acknowledgments

This study was supported in part by JSPS KAKENHI Grant Numbers of 18K19510, and 17H04259.

Conflicts of Interest

Katsuya Maruyama and Katsutoshi Murata are the employee of Siemens Healthcare KK, Tokyo, Japan.

Gregor Körzdörfer, Josef Pfeuffer, and Mathias Nittka are the employee of Siemens Healthcare GmbH, Erlangen, Germany.

The other authors declare that they have no conflicts of interest.

References

1. Deike-Hofmann K, Reuter J, Haase R, et al. Glymphatic pathway of gadolinium-based contrast agents through the brain: overlooked and misinterpreted. Invest Radiol 2019; 54:229–237.
2. Naganawa S, Nakane T, Kawai H, Taoka T. Gd-based contrast enhancement of the perivascular spaces in the basal ganglia. Magn Reson Med Sci 2017; 16:61–65.
3. Naganawa S, Nakane T, Kawai H, Taoka T. Age dependence of gadolinium leakage from the cortical veins into the cerebrospinal fluid assessed with whole brain 3D-real inversion recovery MR imaging. Magn Reson Med Sci 2019; 18:163–169.
4. Naganawa S, Suzuki K, Yamazaki M, Sakurai Y. Serial scans in healthy volunteers following intravenous administration of gadoteridol: time course of contrast enhancement in various cranial fluid spaces. Magn Reson Med Sci 2014; 13:7–13.
5. Naganawa S, Yamazaki M, Kawai H, Sone M, Nakashima T. Contrast enhancement of the anterior eye segment and subarachnoid space: detection in the normal state by heavily T_2-weighted 3D FLAIR. Magn Reson Med Sci 2011; 10:193–199.
6. Kato Y, Bokura K, Taoka T, Naganawa S. Increased signal intensity of low-concentration gadolinium contrast agent by longer repetition time in heavily T_2-weighted-3D-FLAIR. Jpn J Radiol 2019; 37:431–435.
7. Naganawa S, Kawai H, Sone M, Nakashima T. Increased sensitivity to low concentration gadolinium contrast by optimized heavily T_2-weighted 3D-FLAIR to visualize endolymphatic space. Magn Reson Med Sci 2010; 9:73–80.
8. Naganawa S, Kawai H, Taoka T, Sone M. Improved 3D-real inversion recovery: a robust imaging technique for endolymphatic hydrops after intravenous administration of gadolinium. Magn Reson Med Sci 2019; 18:105–108.
9. Naganawa S, Nakane T, Kawai H, et al. Detection of IV-gadolinium leakage from the cortical veins into the CSF using MR fingerprinting. Magn Reson Med Sci 2020; 19:141–146.
10. Kato Y, Ichikawa K, Okudaira K, et al. Comprehensive evaluation of B1(+)-corrected FISP-based magnetic resonance fingerprinting: accuracy, repeatability and reproducibility of T_1 and T_2 relaxation times for ISMRM/NIST system phantom and volunteers. Magn Reson Med Sci 2020; 19:168–175.
11. Badve C, Yu A, Dastmalchian S, et al. MR fingerprinting of adult brain tumors: initial experience. AJNR Am J Neuroradiol 2017; 38:492–499.
12. Buonincontri G, Biagi L, Retico A, et al. Multi-site repeatability and reproducibility of MR fingerprinting of the healthy brain at 1.5 and 3.0 T. Neuroimage 2019; 195:362–372.
13. Körzdörfer G, Kirsch R, Liu K, et al. Reproducibility and repeatability of MR fingerprinting relaxometry in the human brain. Radiology 2019; 292:429–437.
14. Naganawa S, Ito R, Taoka T, Yoshida T, Sone M. The space between the pial sheath and the cortical venous wall may connect to the meningeal lymphatics. Magn Reson Med Sci 2020; 19:1–4.

15. Ohashi T, Naganawa S, Katagiri T, Kuno K. Relationship between contrast enhancement of the perivascular space in the basal ganglia and endolymphatic volume ratio. Magn Reson Med Sci 2018; 17:67–72.
16. Berger F, Kubik-Huch RA, Niemann T, et al. Gadolinium distribution in cerebrospinal fluid after administration of a gadolinium-based MR contrast agent in humans. Radiology 2018; 288:703–709.
17. Freeze WM, Schnerr RS, Palm WM, et al. Pericortical enhancement on delayed postgadolinium fluid-attenuated inversion recovery images in normal aging, mild cognitive impairment, and Alzheimer disease. AJNR Am J Neuroradiol 2017; 38:1742–1747.
18. Naganawa S, Yamazaki M, Kawai H, Bokura K, Sone M, Nakashima T. Visualization of endolymphatic hydrops in Meniere's disease after single-dose intravenous gadolinium-based contrast medium: timing of optimal enhancement. Magn Reson Med Sci 2012; 11:43–51.
19. Naganawa S, Yamazaki M, Kawai H, Bokura K, Sone M, Nakashima T. Visualization of endolymphatic hydrops in Meniere's disease with single-dose intravenous gadolinium-based contrast media using heavily T(2)-weighted 3D-FLAIR. Magn Reson Med Sci 2010; 9:237–242.
20. Jost G, Frenzel T, Lohrke J, Lenhard DC, Naganawa S, Pietsch H. Penetration and distribution of gadolinium-based contrast agents into the cerebrospinal fluid in healthy rats: a potential pathway of entry into the brain tissue. Eur Radiol 2017; 27:2877–2885.
21. Nation DA, Sweeney MD, Montagne A, et al. Blood-brain barrier breakdown is an early biomarker of human cognitive dysfunction. Nat Med 2019; 25:270–276.
22. van de Haar HJ, Burgmans S, Jansen JFA, et al. Blood-brain barrier leakage in patients with early Alzheimer disease. Radiology 2016; 281:527–535.
23. Iliff JJ, Lee H, Yu M, et al. Brain-wide pathway for waste clearance captured by contrast-enhanced MRI. J Clin Invest 2013; 123:1299–1309.
24. Rasmussen MK, Mestre H, Nedergaard M. The glymphatic pathway in neurological disorders. Lancet Neurol 2018; 17:1016–1024.
25. Taoka T, Naganawa S. Glymphatic imaging using MRI. J Magn Reason Imaging 2020; 51:11–24.
26. Chatterjee K, Carman-Esparza CM, Munson JM. Methods to measure, model and manipulate fluid flow in brain. J Neurosci Methods 2020; 333:108541.
27. Taoka T, Naganawa S. Gadolinium-based contrast media, cerebrospinal fluid and the glymphatic system: possible mechanisms for the deposition of gadolinium in the brain. Magn Reson Med Sci 2018; 17:111–119.
28. Eide PK, Ringstad G. MRI with intrathecal MRI gadolinium contrast medium administration: a possible method to assess glymphatic function in human brain. Acta Radiol Open 2015; 4:2058460115609635.
29. Provenzano DA, Pellis Z, DeRiggi L. Fatal gadolinium-induced encephalopathy following accidental intrathecal administration: a case report and a comprehensive evidence-based review. Reg Anesth Pain Med 2019. doi: 10.1136/rapm-2019-100422. [Epub ahead of print].
30. Ma D, Gulani V, Seiberlich N, et al. Magnetic resonance fingerprinting. Nature 2013; 495:187–192.
31. Körzdörfer G, Kluge T, Pfeuffer, J, et al. Spatial biases in magnetic resonance fingerprinting parameter maps arising from undersampling patterns. Proceedings of the 25th Annual Meeting of ISMRM, Honolulu, 2017; 3956.
32. Pfeuffer J, Kechagias A, Körzdörfer G, Ma D, Griswold M, Nittka M. Mitigation of spiral undersampling artifacts in magnetic resonance fingerprinting (MRF) by adapted interleaf reordering. Proceedings of the 25th Annual Meeting of ISMRM, Honolulu, 2017; 133.
33. Chung S, Kim D, Breton E, Axel L. Rapid B1+ mapping using a preconditioning RF pulse with TurboFLASH readout. Magn Reson Med 2010; 64:439–446.
34. van der Kouwe AJ, Benner T, Fischl B, et al. On-line automatic slice positioning for brain MR imaging. Neuroimage 2005; 27:222–230.
35. Naganawa S, Komada T, Fukatsu H, Ishigaki T, Takizawa O. Observation of contrast enhancement in the cochlear fluid space of healthy subjects using a 3D-FLAIR sequence at 3 Tesla. Eur Radiol 2006; 16:733–737.
36. Edeklev CS, Halvorsen M, Lovland G, et al. Intrathecal use of gadobutrol for glymphatic MR imaging: prospective safety study of 100 patients. AJNR Am J Neuroradiol 2019; 40:1257–1264.
37. Eide PK, Ringstad G. *In vivo* imaging of molecular clearance from human entorhinal cortex: a possible method for preclinical testing of dementia. Gerontol Geriatr Med 2019; 5:2333721419889739.
38. Eide PK, Valnes LM, Pripp AH, Mardal KA, Ringstad G. Delayed clearance of cerebrospinal fluid tracer from choroid plexus in idiopathic normal pressure hydrocephalus. J Cereb Blood Flow Metab 2019:271678X19874790.
39. Eide PK, Vatnehol SAS, Emblem KE, Ringstad G. Magnetic resonance imaging provides evidence of glymphatic drainage from human brain to cervical lymph nodes. Sci Rep 2018; 8:7194.
40. Ringstad G, Valnes LM, Dale AM, et al. Brain-wide glymphatic enhancement and clearance in humans assessed with MRI. JCI Insight 2018; 3:e121537.
41. Nehra AK, McDonald RJ, Bluhm AM, et al. Accumulation of gadolinium in human cerebrospinal fluid after Gadobutrol-enhanced MR imaging: a prospective observational cohort study. Radiology 2018; 288:416–423.
42. Samardzic D, Thamburaj K. Magnetic resonance characteristics and susceptibility weighted imaging of the brain in gadolinium encephalopathy. J Neuroimaging 2015; 25:136–139.
43. Li K-L, Jackson A. New hybrid technique for accurate and reproducible quantitation of dynamic contrast-enhanced MRI data. Magn Reson Med 2003; 50:1286–1295.
44. van de Haar HJ, Jansen JFA, Jeukens CRLPN, et al. Subtle blood-brain barrier leakage rate and spatial extent: Considerations for dynamic contrast-enhanced MRI. Med Phys 2017; 44:4112–4125.
45. Ma D, Jiang Y, Chen Y, et al. Fast 3D magnetic resonance fingerprinting for a whole-brain coverage. Magn Reson Med 2018; 79:2190–2197.
46. Ma D, Jones SE, Deshmane A, et al. Development of high-resolution 3D MR fingerprinting for detection and characterization of epileptic lesions. J Magn Reson Imaging 2019; 49:1333–1346.